Supporting Information

Integrated Continuous Plug-Flow Crystallization and Spray Drying of Pharmaceuticals for Dry Powder Inhalation

Gabriela Daisy Hadiwinoto[1], Philip C.L. Kwok[2], Henry H.Y. Tong[3], Si Nga Wong[4], Shing Fung Chow[4], Richard Lakerveld[1]*

[1] Department of Chemical and Biological Engineering, The Hong Kong University of Science and Technology, Clear Water Bay, Kowloon, Hong Kong

[2] Sydney Pharmacy School, Faculty of Medicine and Health, The University of Sydney, New South Wales 2006, Australia

[3] School of Health Sciences, Macao Polytechnic Institute, R. de Luis Gonzaga Gomes, Macau

[4] Department of Pharmacology and Pharmacy, The University of Hong Kong, 21 Sassoon Road, Pokfulam, Hong Kong

Calculation of the NGI cut-off diameter (Table 4 in manuscript)

The cut-off diameters of the various stages in the NGI are calculated with the following equation:

$$D_{50,Q,i} = D_{50,Qn,i}\left(\frac{Q_n}{Q}\right)^{x_i},$$

Where $D_{50,,i}$ is the cut-off diameter of nozzle stage i at a reference value of airflow rate (Q_n = 60 L/min) and x_i is a specific exponent value for nozzle stage i.

Nozzle stage (i)	$D_{50,Qn,i}$ (L/min)	x_i
1		
2	8.06	0.54
3	4.46	0.52
4	2.82	0.50
5	1.66	0.47
6	0.94	0.53
7	0.55	0.60
8	0.34	0.67

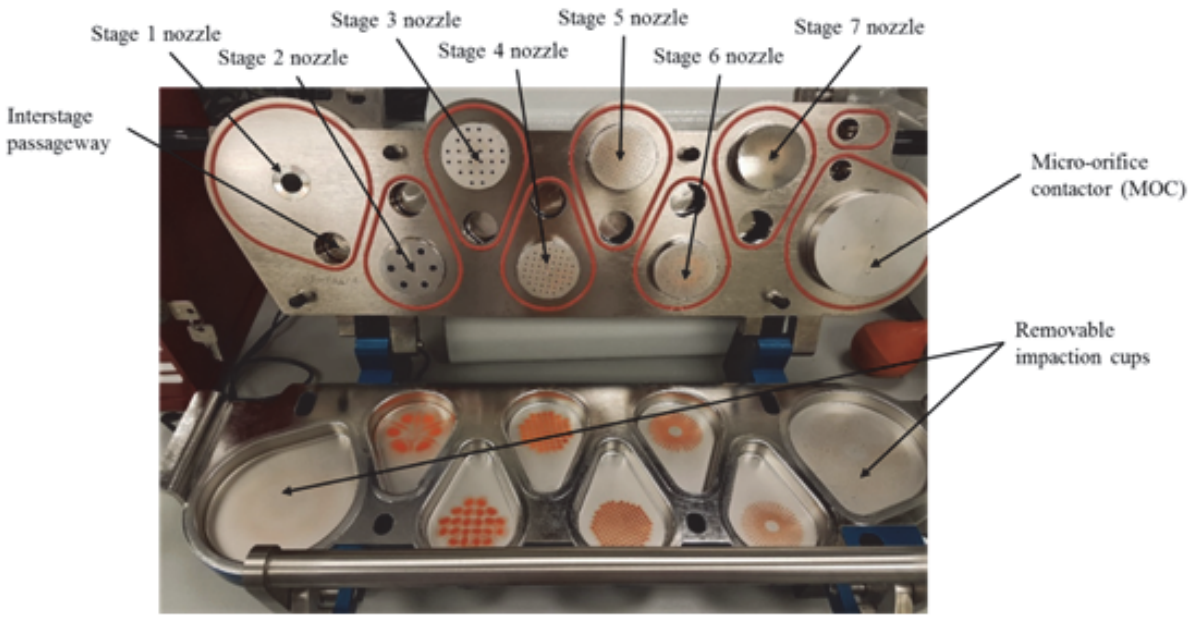

Figure S1. Next Generation Impactor^{TM} for particle deposition tests (see Table S4 for corresponding cut-off diameters).

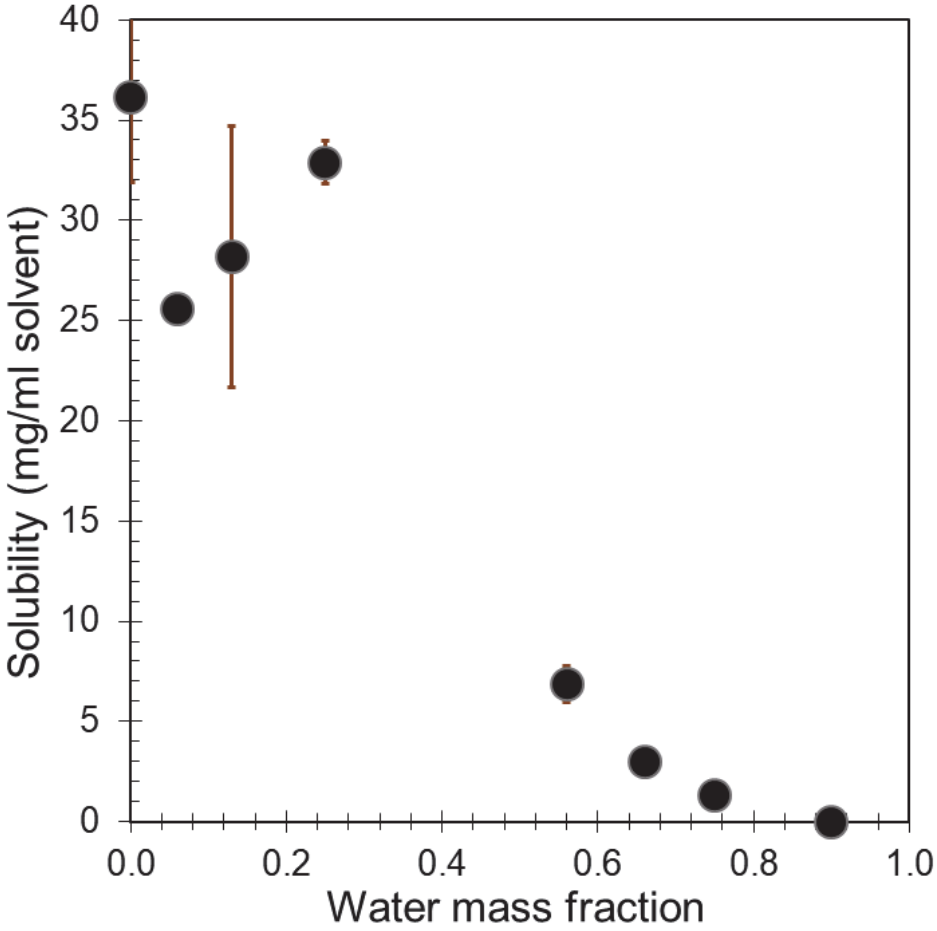

Figure S2. Solubility of rifapentine in an acetone-water mixture at 50°C. The error bars represent the standard deviation of repeated experiments. All experiments were conducted in triplicate except the experiments with a water fraction of 6%, 75%, and 90%, which were conducted once.

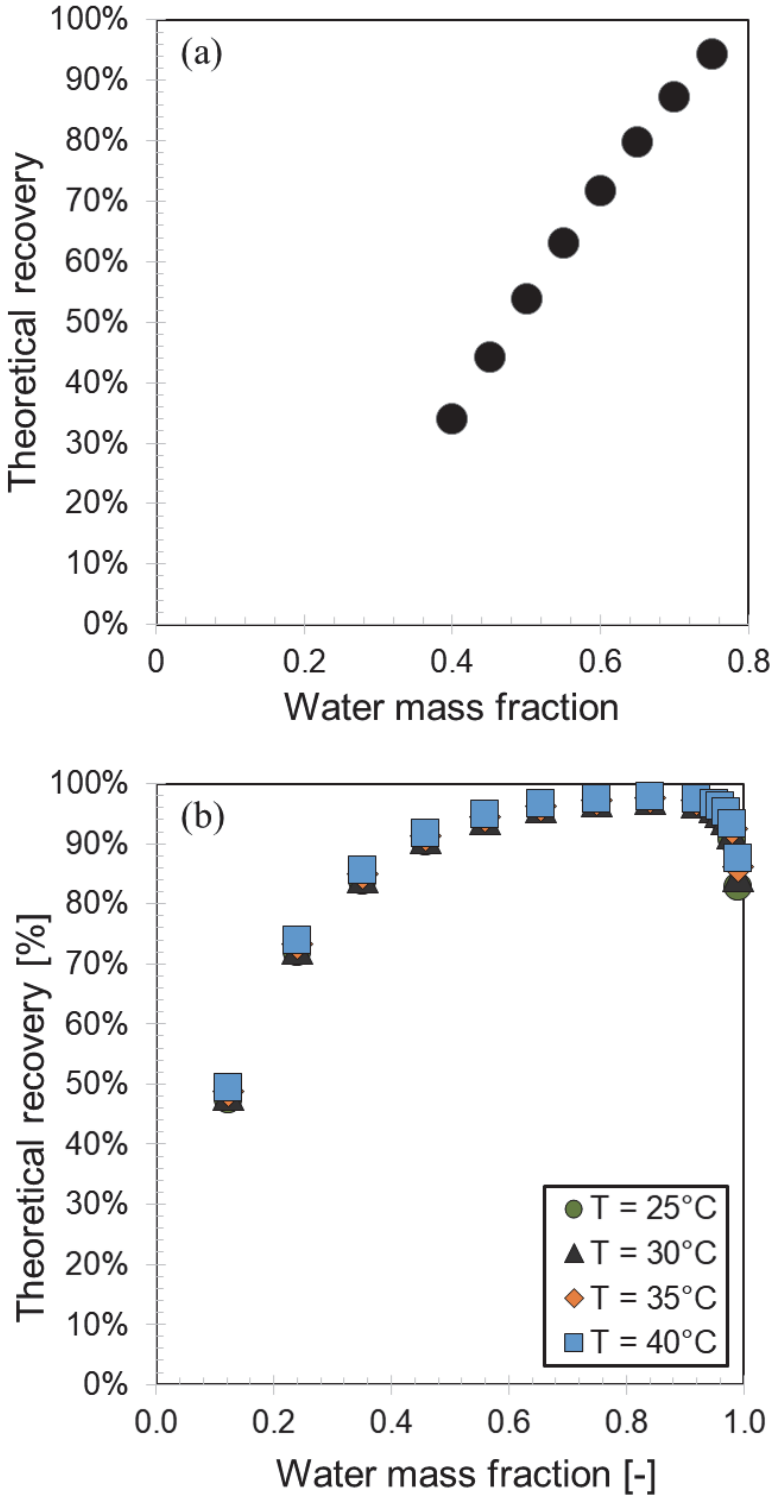

Figure S3. Theoretical recovery of APIs as a function of final water mass fraction. a) Rifapentine (feed solvent is a mixture of acetone and water in a mass ratio of 3:1, T = 50°C), b) Beclomethasone dipropionate (feed solvent is ethanol, various temperatures)

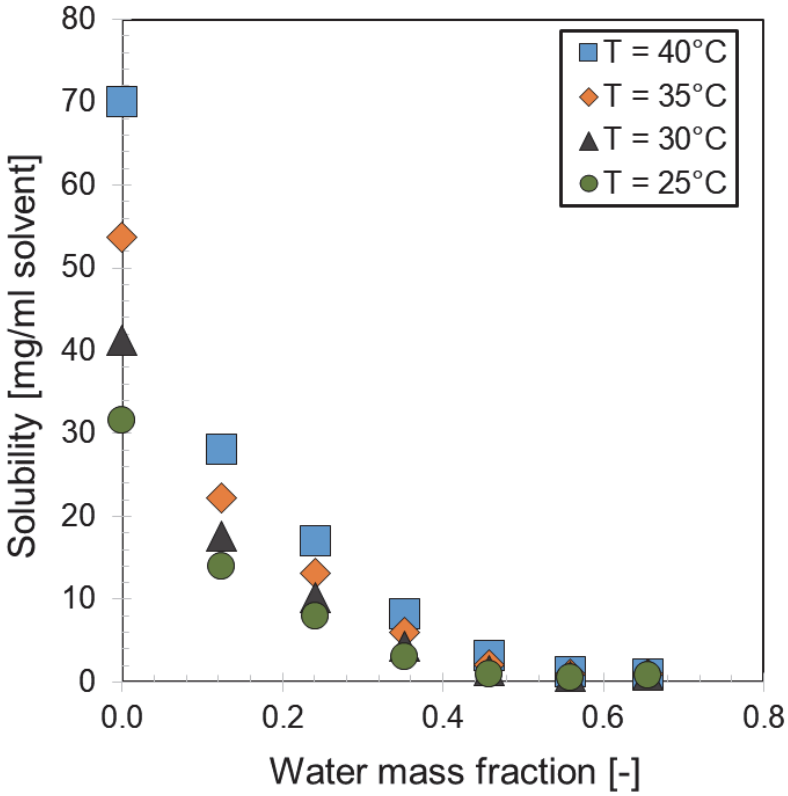

Figure S4. Solubility of beclomethasone dipropionate in an ethanol-water system at various temperatures. All experiments were conducted once.

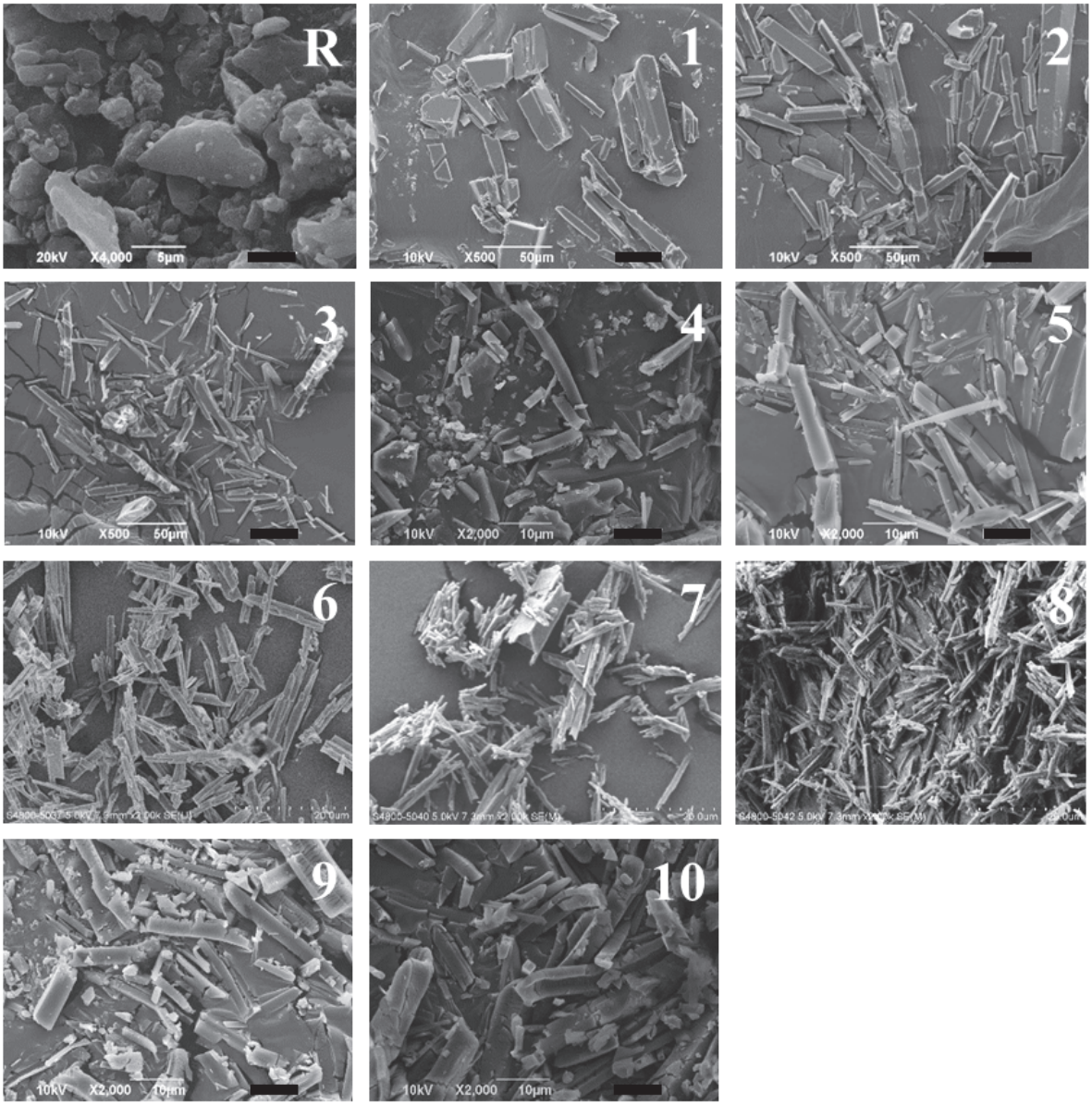

Figure S5. SEM images of the crystallized beclometasone dipropionate from each stand-alone continuous crystallization experiment (see Table S5 for conditions) and raw material ("R"). Note that different scale bars are used.

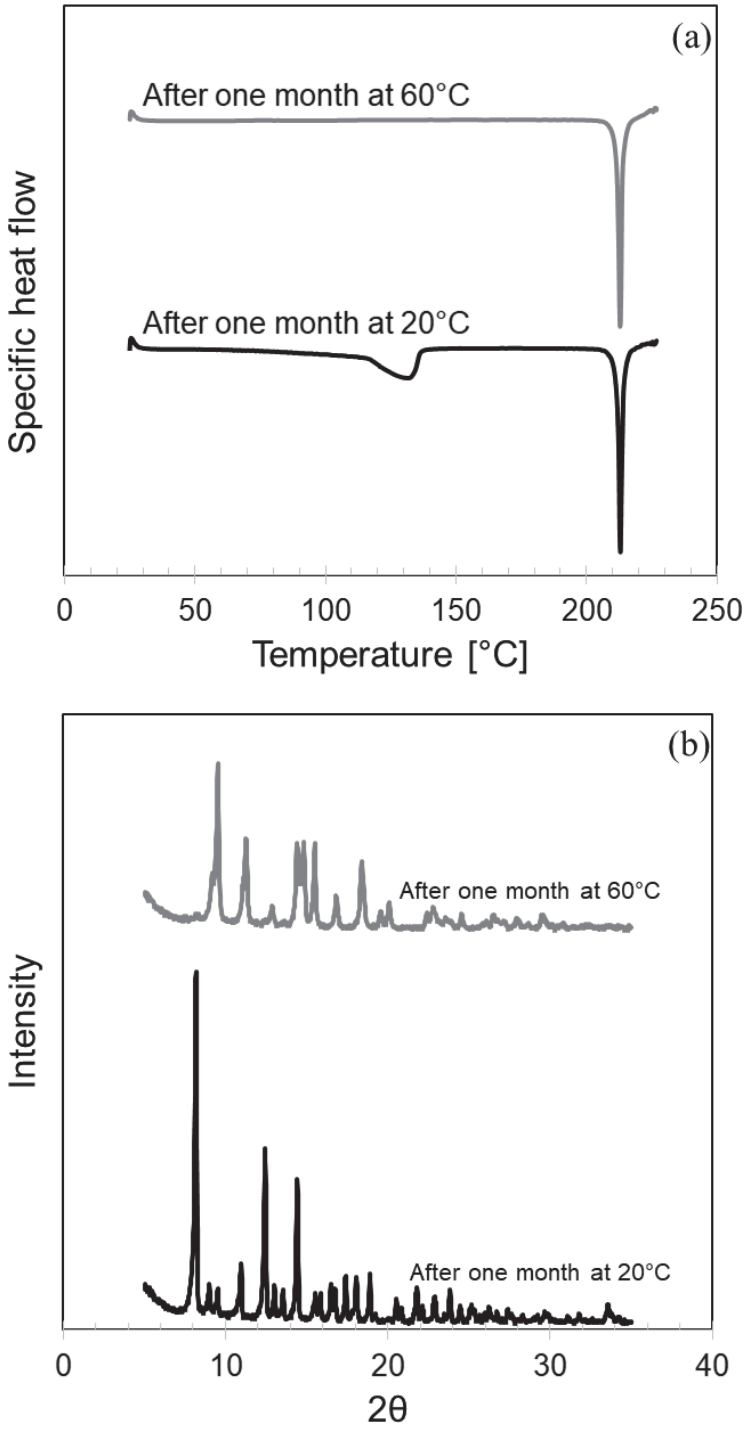

Figure S6. Stability tests of produced beclometasone dipropionate crystals at room temperature, relative humidity between 35% and 40%, and elevated temperature (T = 60°C). a) DSC profiles after one month. b) XRD diagrams after one month. Note that the solid-state form after one month at room temperature has not changed, whereas a solid-state transition, most likely from the monohydrate to the anhydrate form, occurs at elevated temperature within one month.

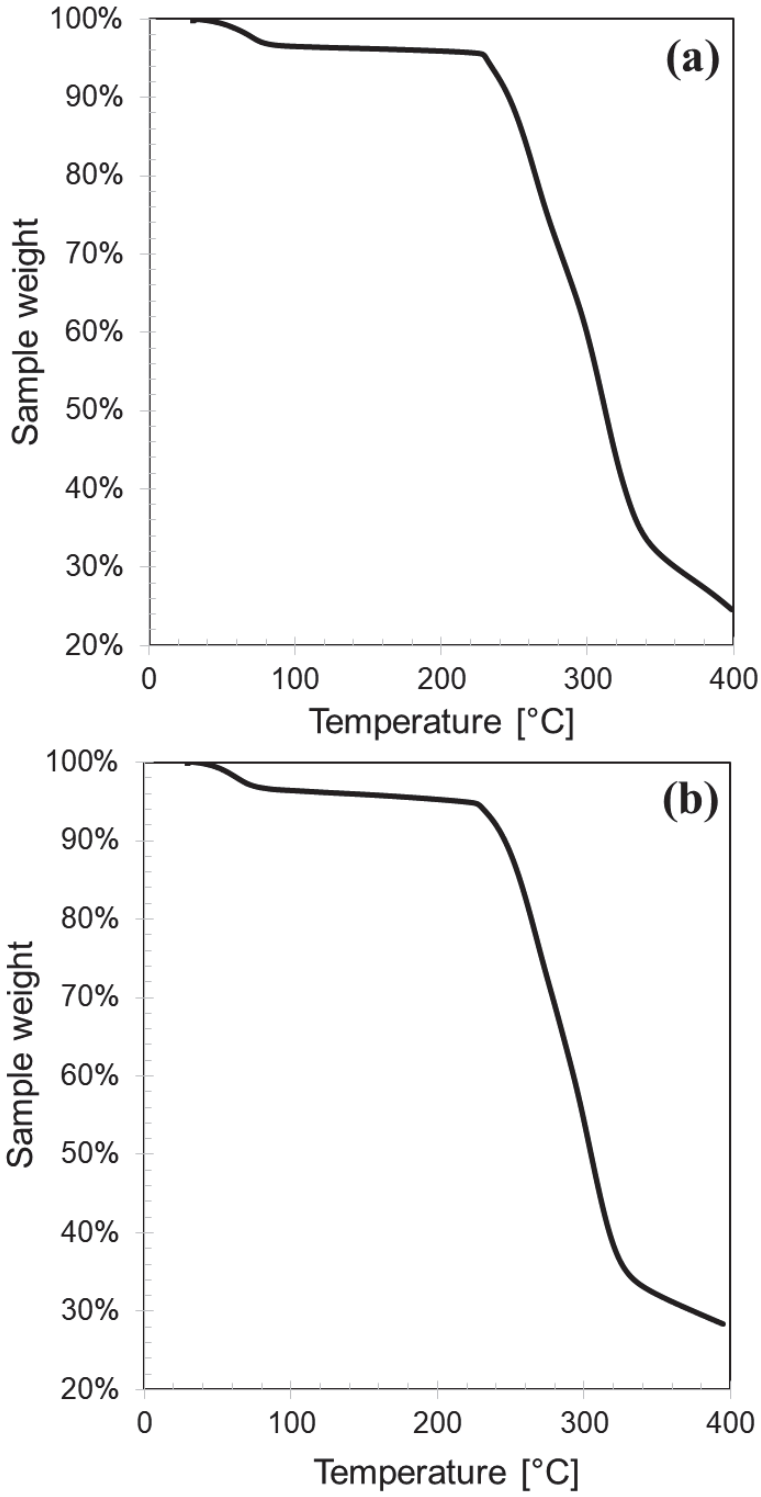

Figure S7. TGA profiles of beclometasone dipropionate. a) vacuum-dried powder, b) spray-dried powder from stand-alone spray drying experiments

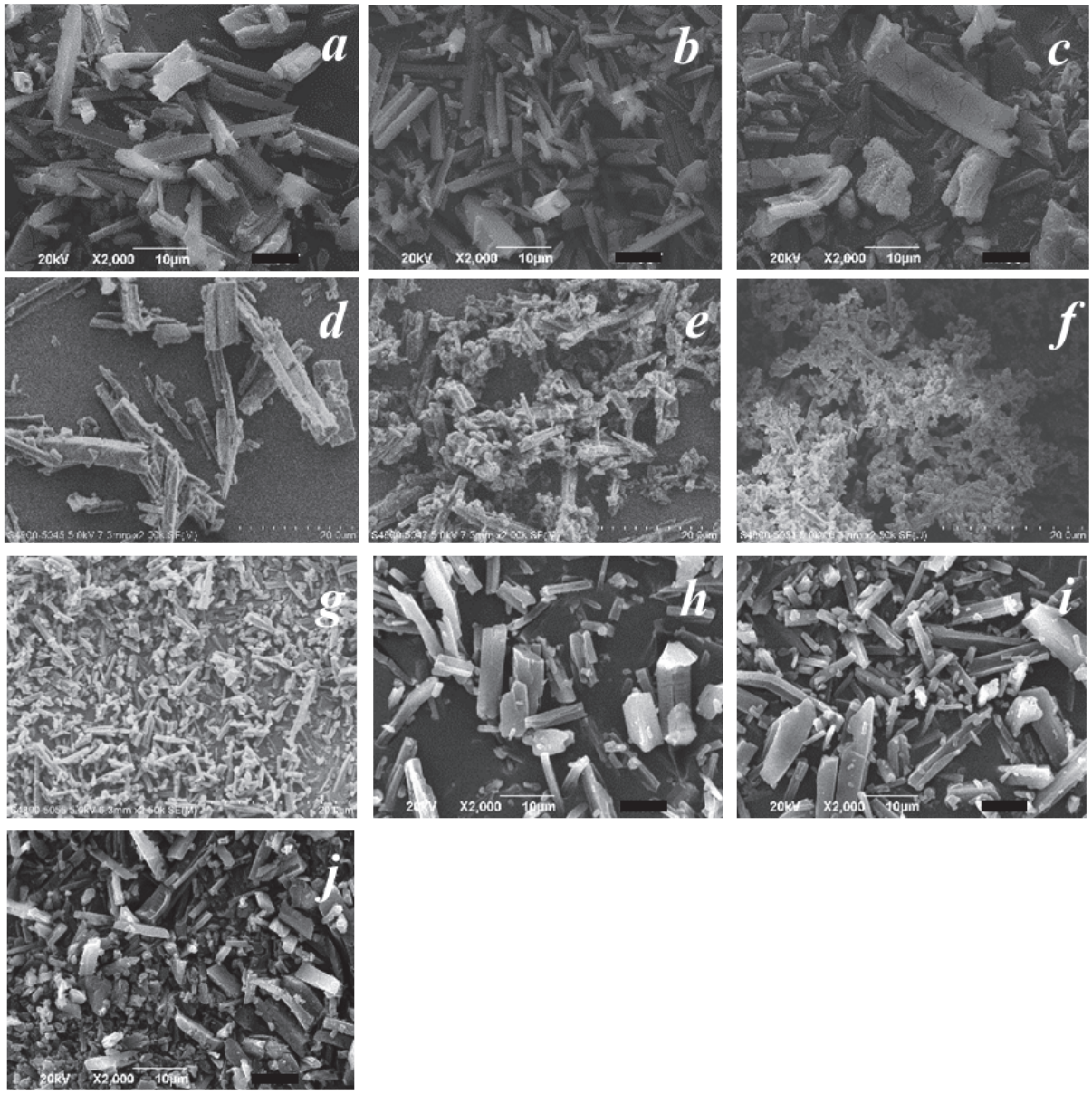

Figure S8. SEM images of the dried beclomethasone dipropionate from stand-alone spray drying experiments using crystals obtained from continuous crystallization experiments (see Table 3) as feed material. Note that different scale bars are used. Estimated particle dimensions are given in Table S6.

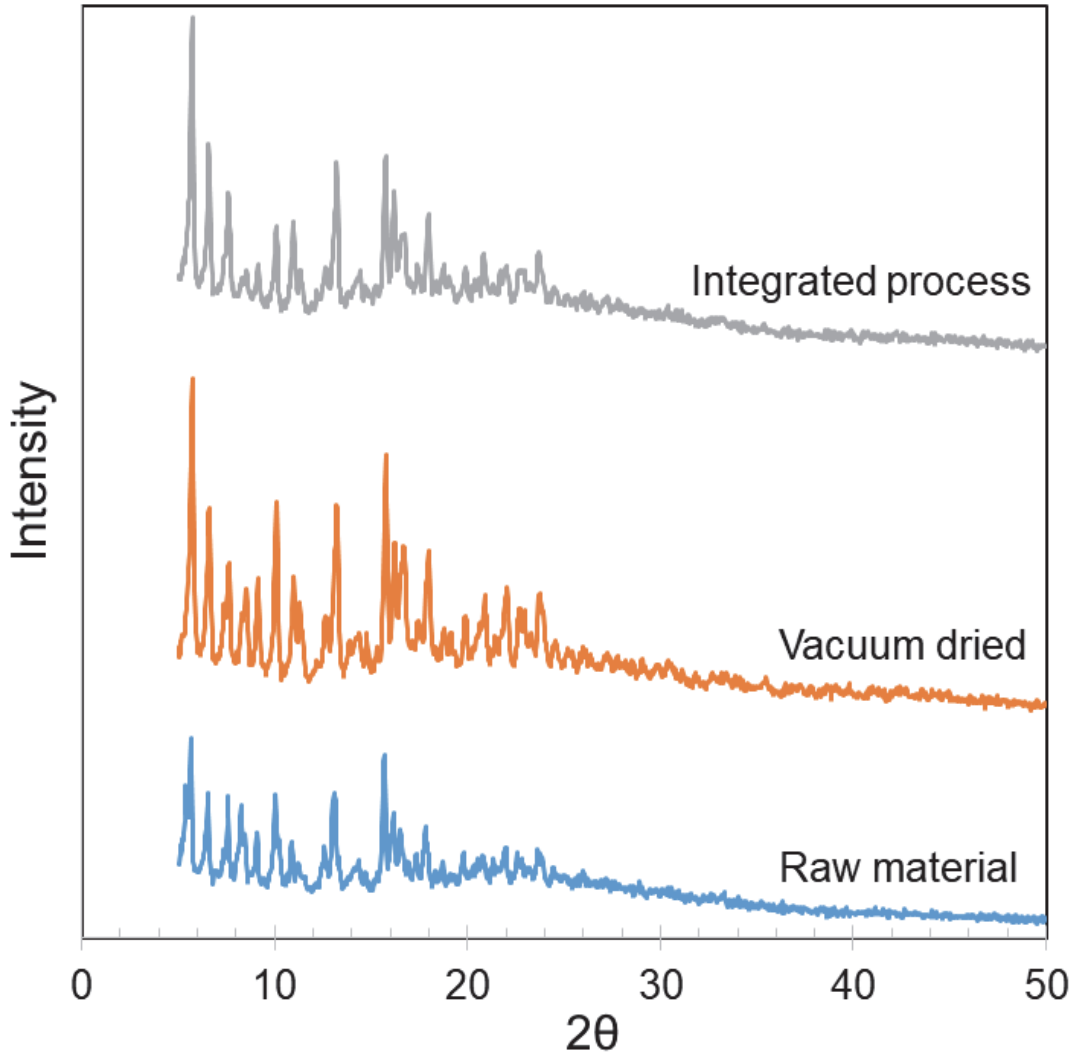

Figure S9. Powder XRD spectra of rifapentine produced from the raw material, vacuum dried powder, and powder obtained from the integrated process.

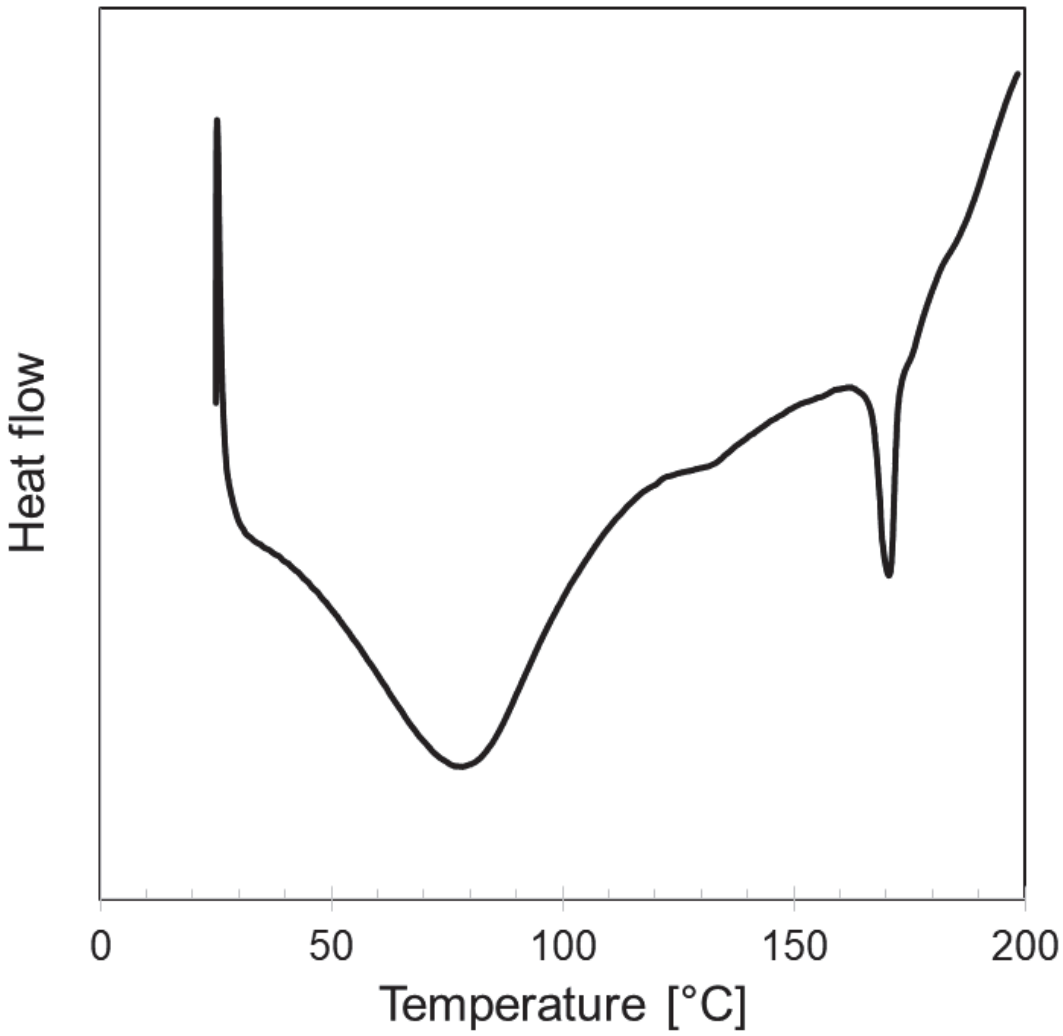

Figure S10. DSC profile of the rifapentine powder obtained from the integrated process.

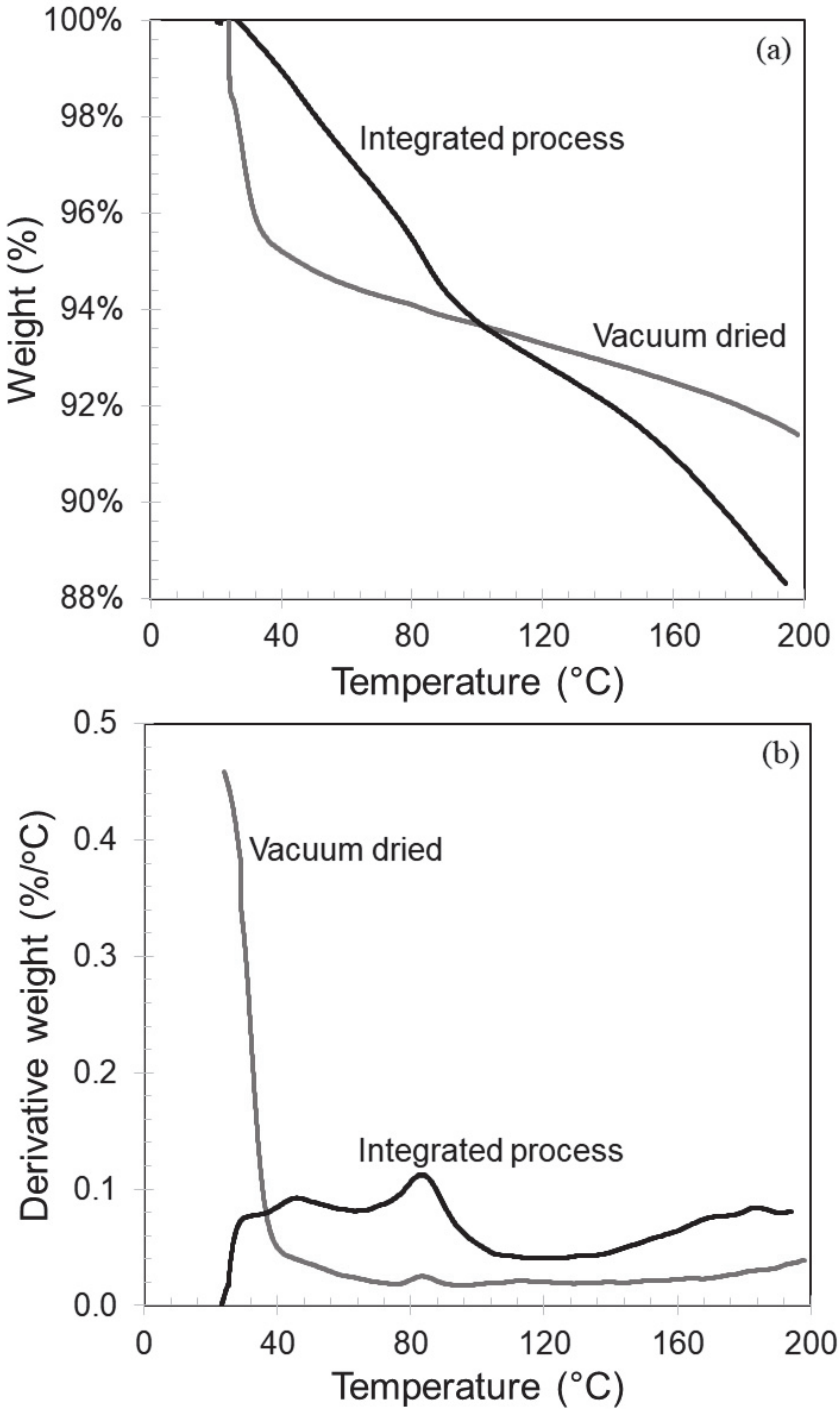

Figure S11. TGA profiles of the rifapentine powder obtained from crystallization followed by vacuum drying and from the integrated process. a) absolute weight loss, b) derivative of the weight loss. Note that after the release of acetone at low temperature, a small maximum in the derivative weight can be seen just before 100°C, which is expected to be the release of water. For both samples, the weight has decreased approximately 6% up to 100°C, which is believed to be the total solvent content.

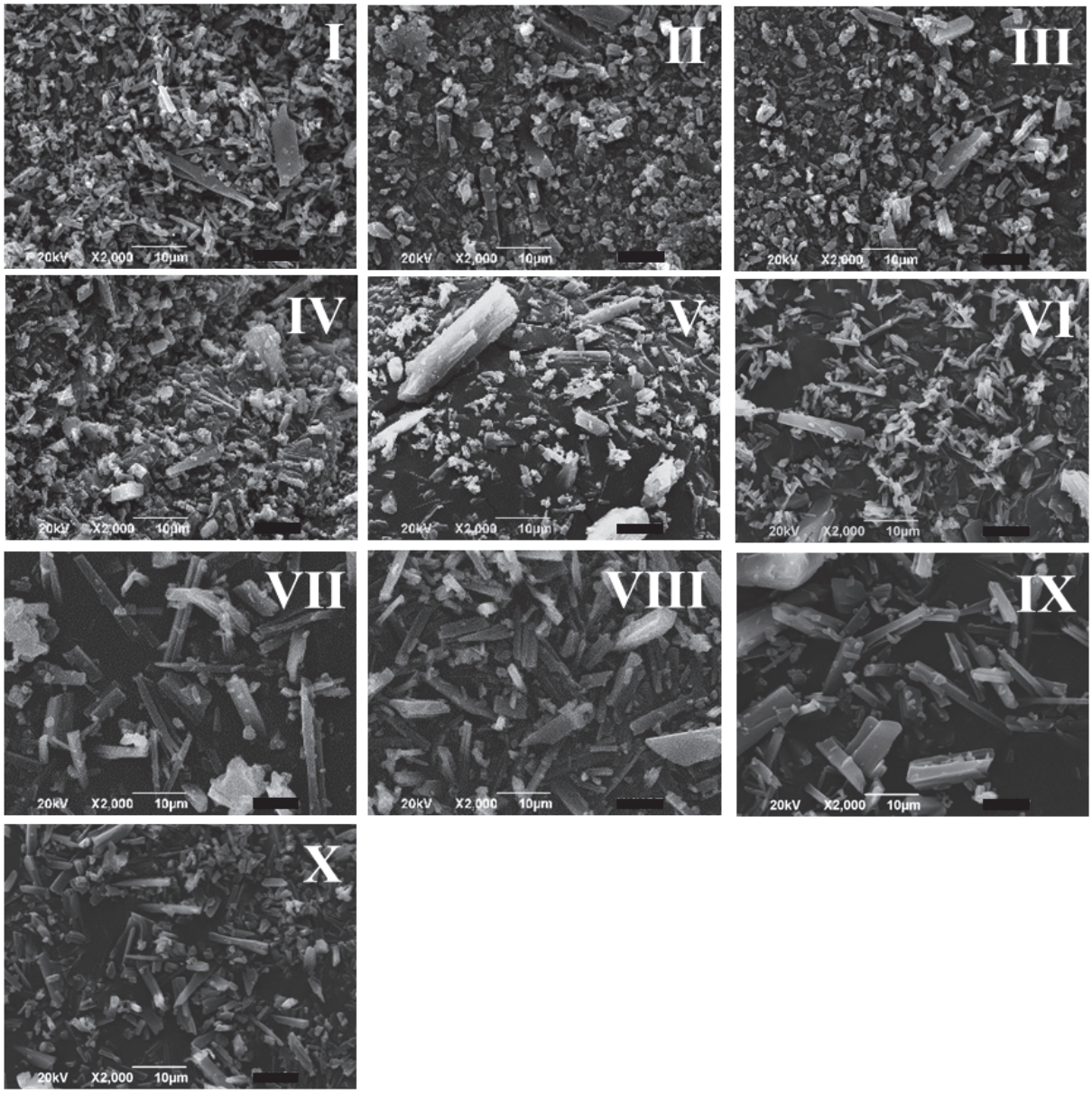

Figure S12. SEM images of the beclometasone dipropionate crystals produced with the integrated process (see Table 4 for operating conditions).

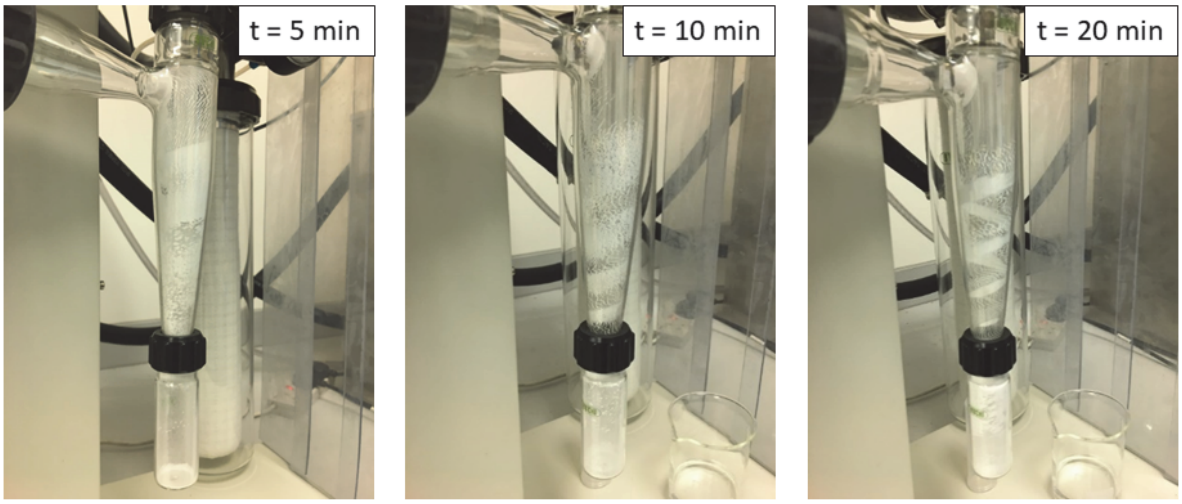

Figure S13. Beclometasone dipropionate powder adhesion in the cyclone of the spray dryer as function of time (observed during Experiment II, see Table 4 for operating conditions).

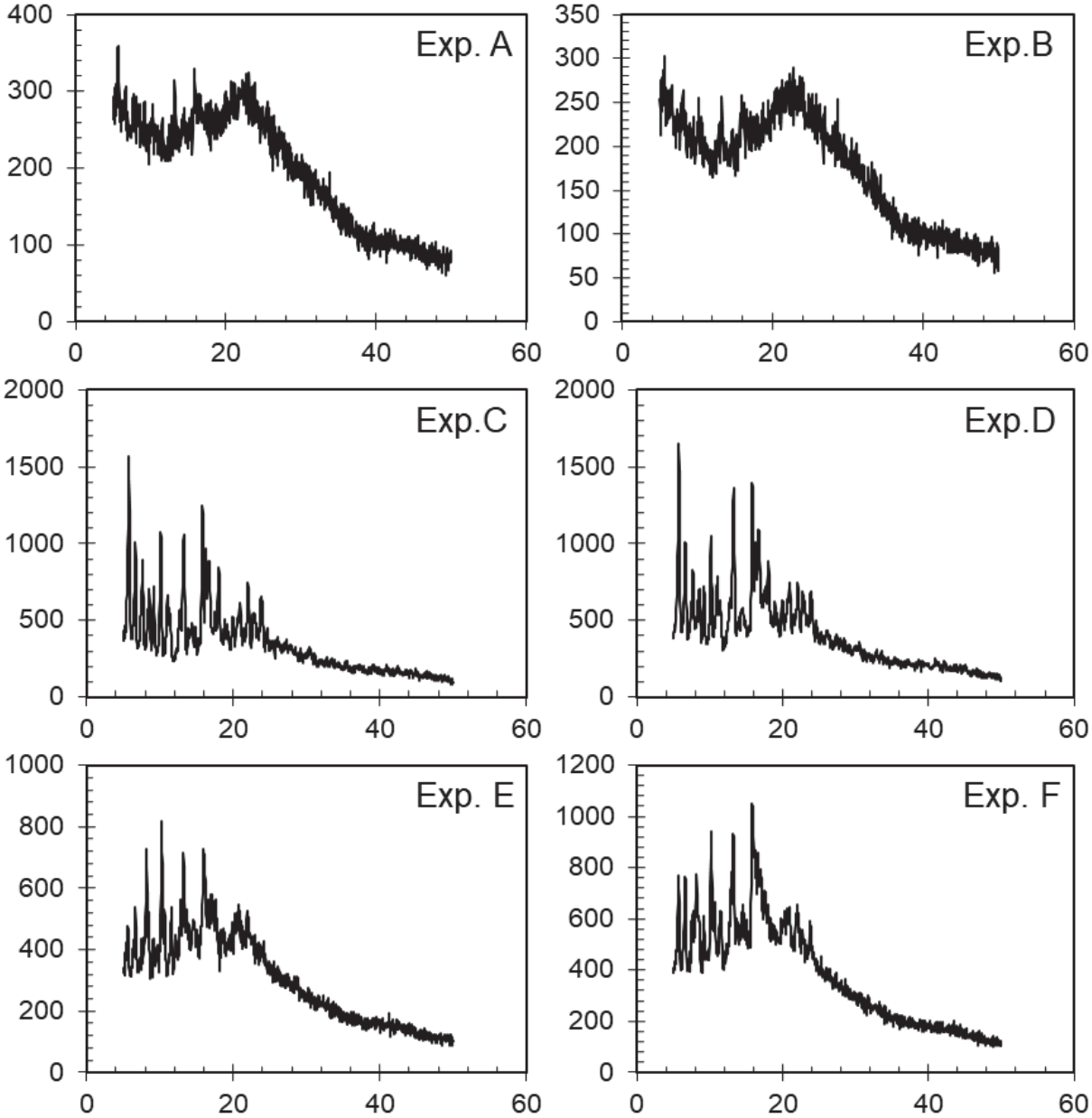

Figure S14. XRD pattern of rifapentine powder obtained from stand-alone crystallization experiments. The horizontal axis is two times the angle of diffraction (2θ) and the vertical axis is the intensity.

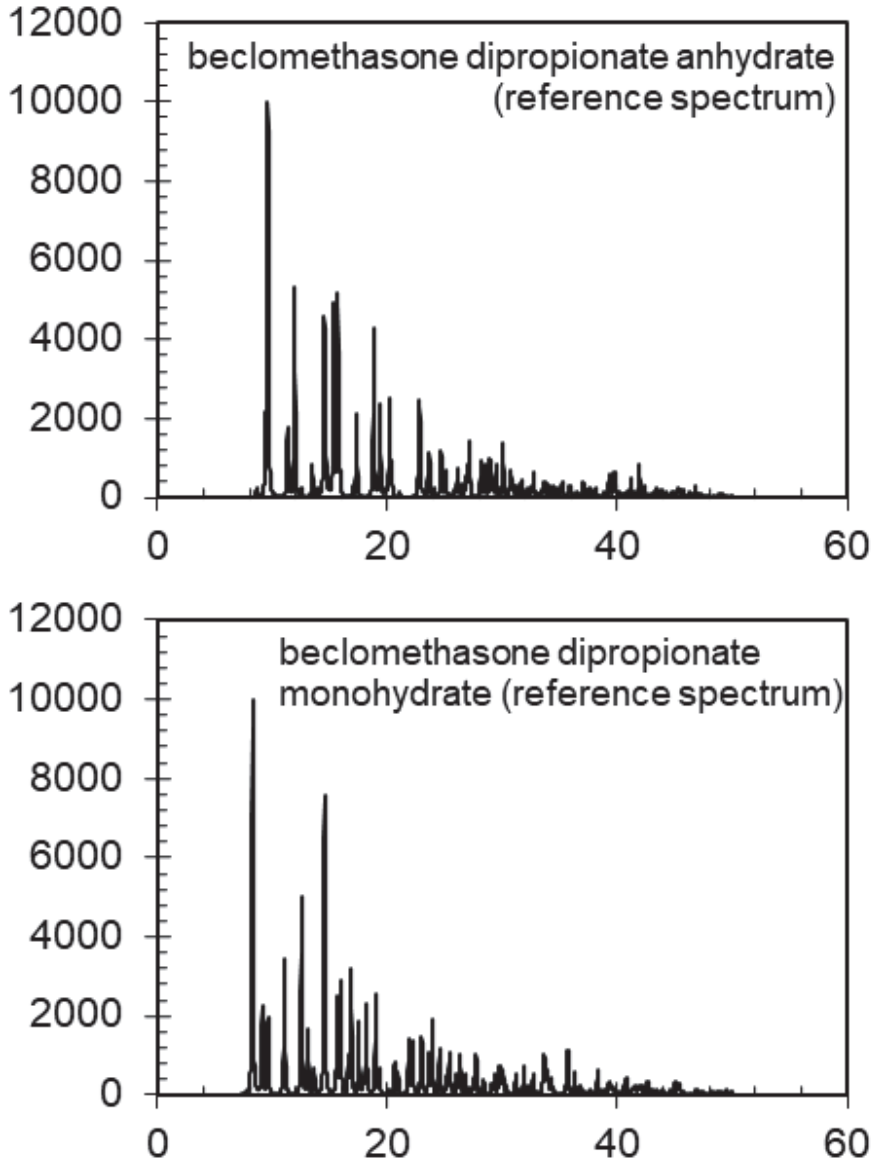

Figure S15. XRD patterns of different solid-state forms of beclomethasone dipropionate. The horizontal axis is two times the angle of diffraction (2θ) and the vertical axis is the intensity.

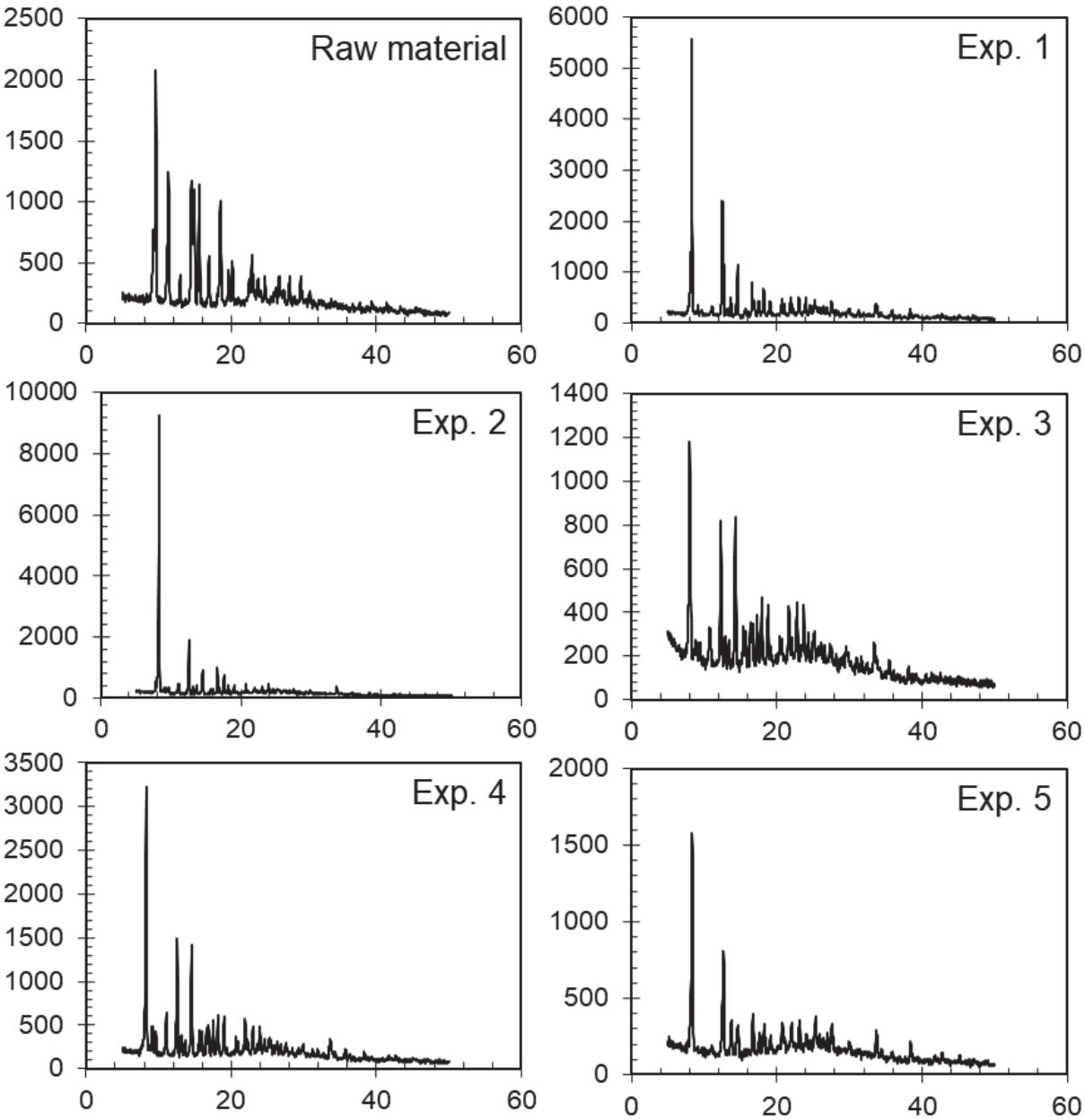

Figure S16. XRD pattern of beclomethasone dipropionate powder obtained from stand-alone crystallization experiments. The horizontal axis is two times the angle of diffraction (2θ) and the vertical axis is the intensity.

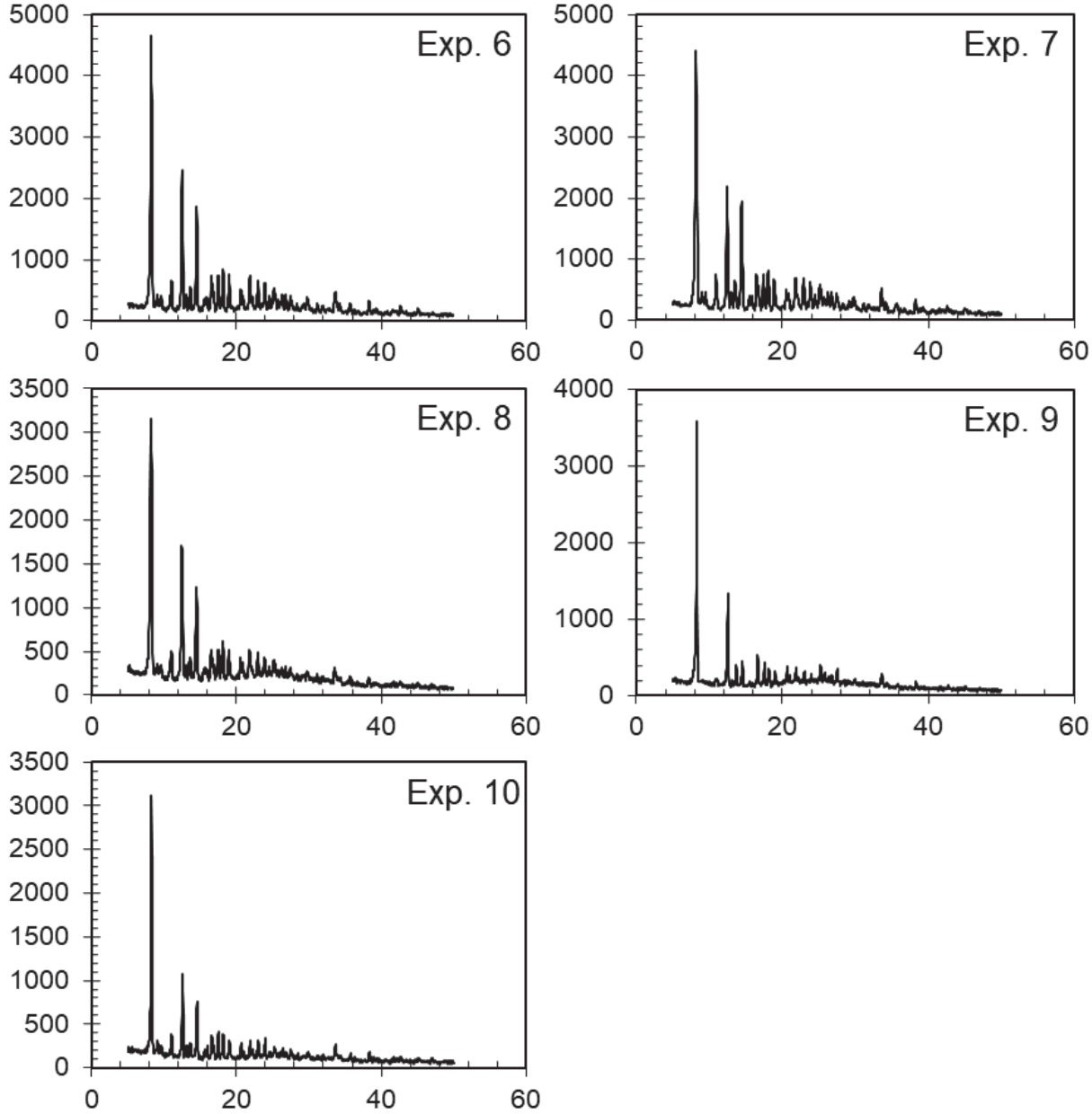

Figure S17. XRD pattern of beclomethasone dipropionate powder obtained from stand-alone crystallization experiments. The horizontal axis is two times the angle of diffraction (2θ) and the vertical axis is the intensity.

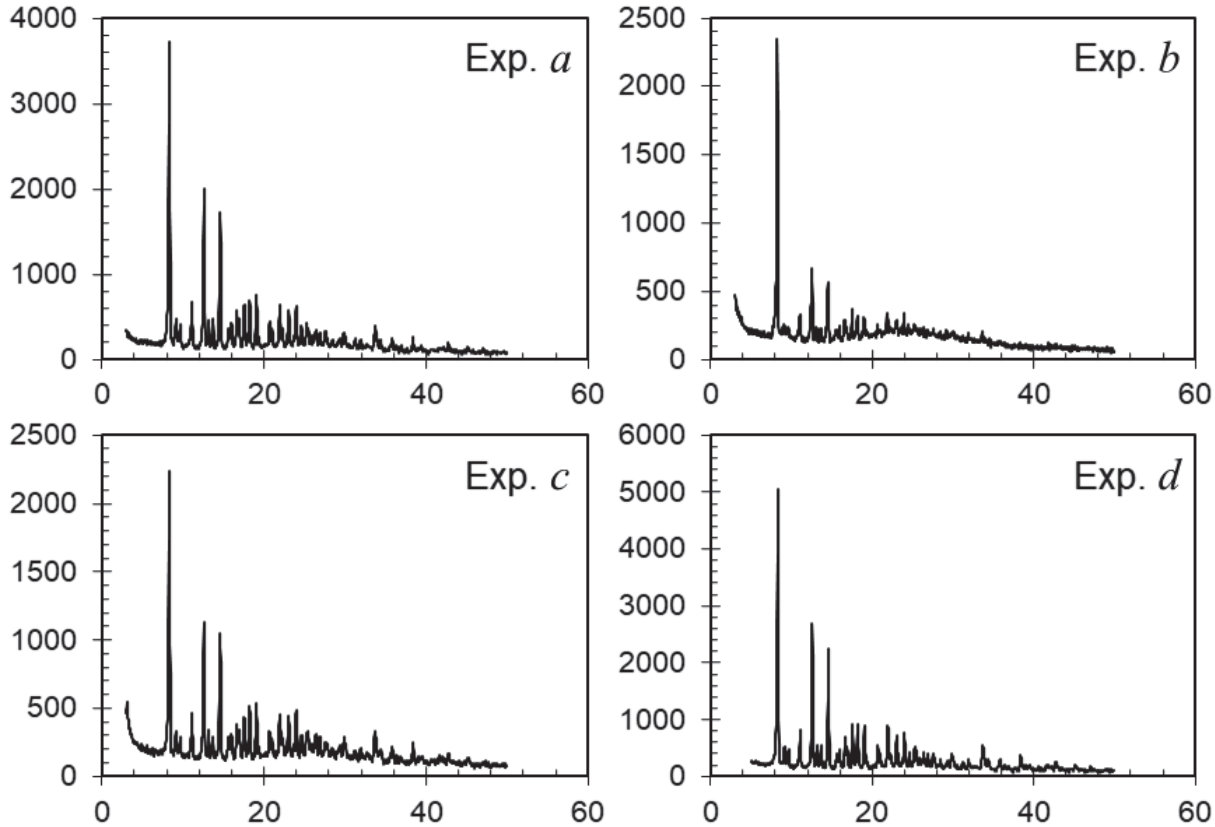

Figure S18. XRD pattern of beclomethasone dipropionate powder obtained from stand-alone spray drying experiments. The horizontal axis is two times the angle of diffraction (2θ) and the vertical axis is the intensity.

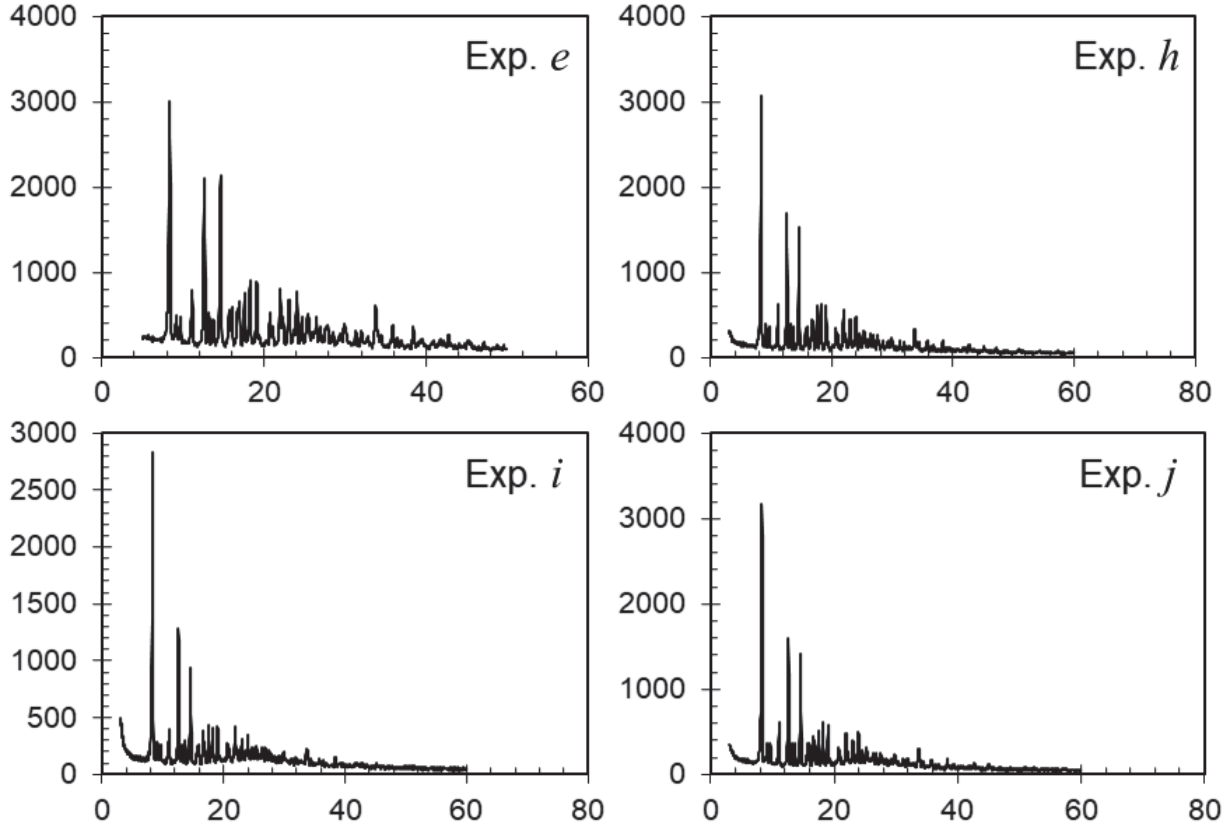

Figure S19. XRD pattern of beclomethasone dipropionate powder obtained from stand-alone spray drying experiments. The horizontal axis is two times the angle of diffraction (2θ) and the vertical axis is the intensity.

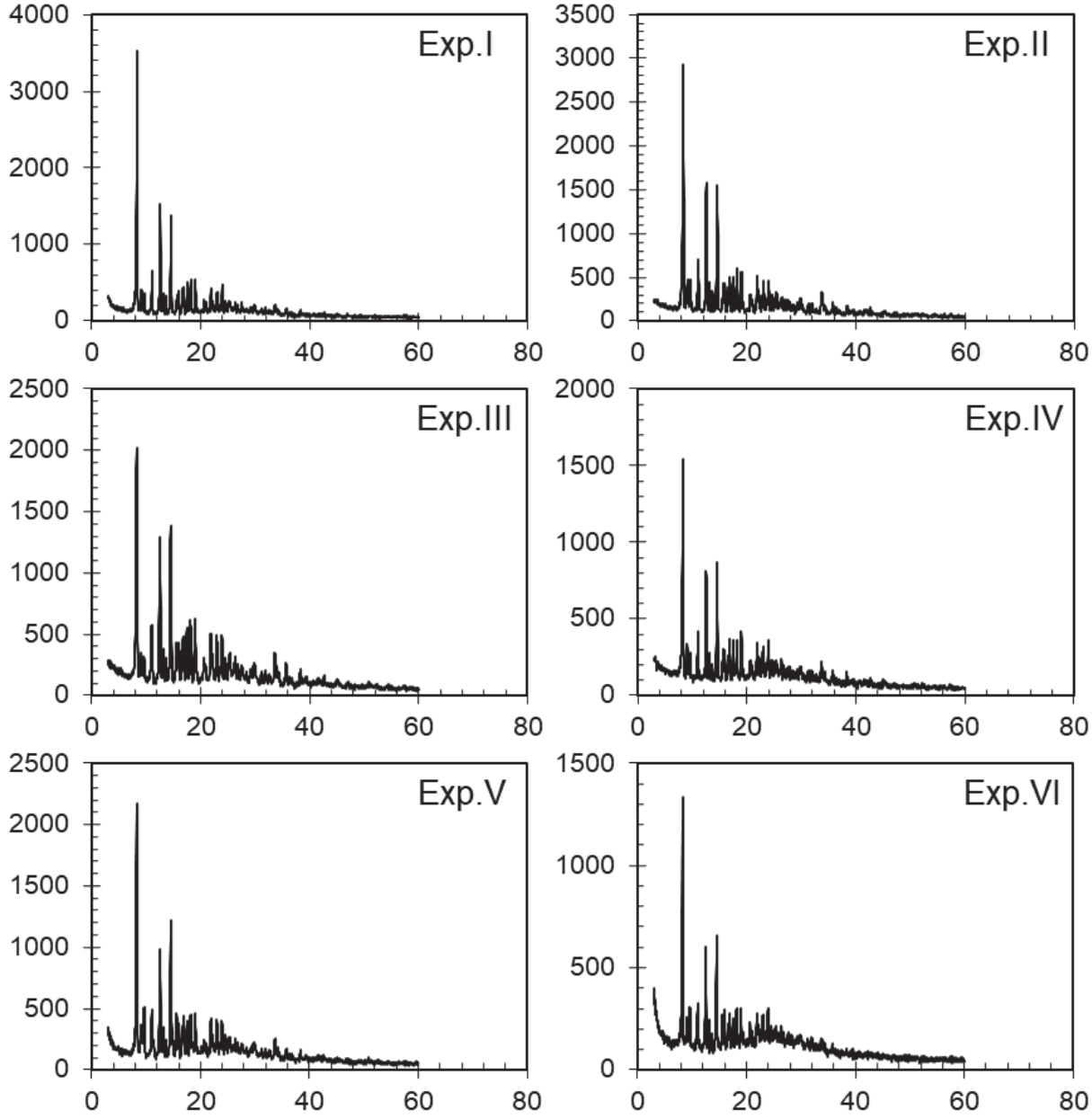

Figure S20. XRD pattern of beclomethasone dipropionate powder obtained from the integrated process. The horizontal axis is two times the angle of diffraction (2θ) and the vertical axis is the intensity.

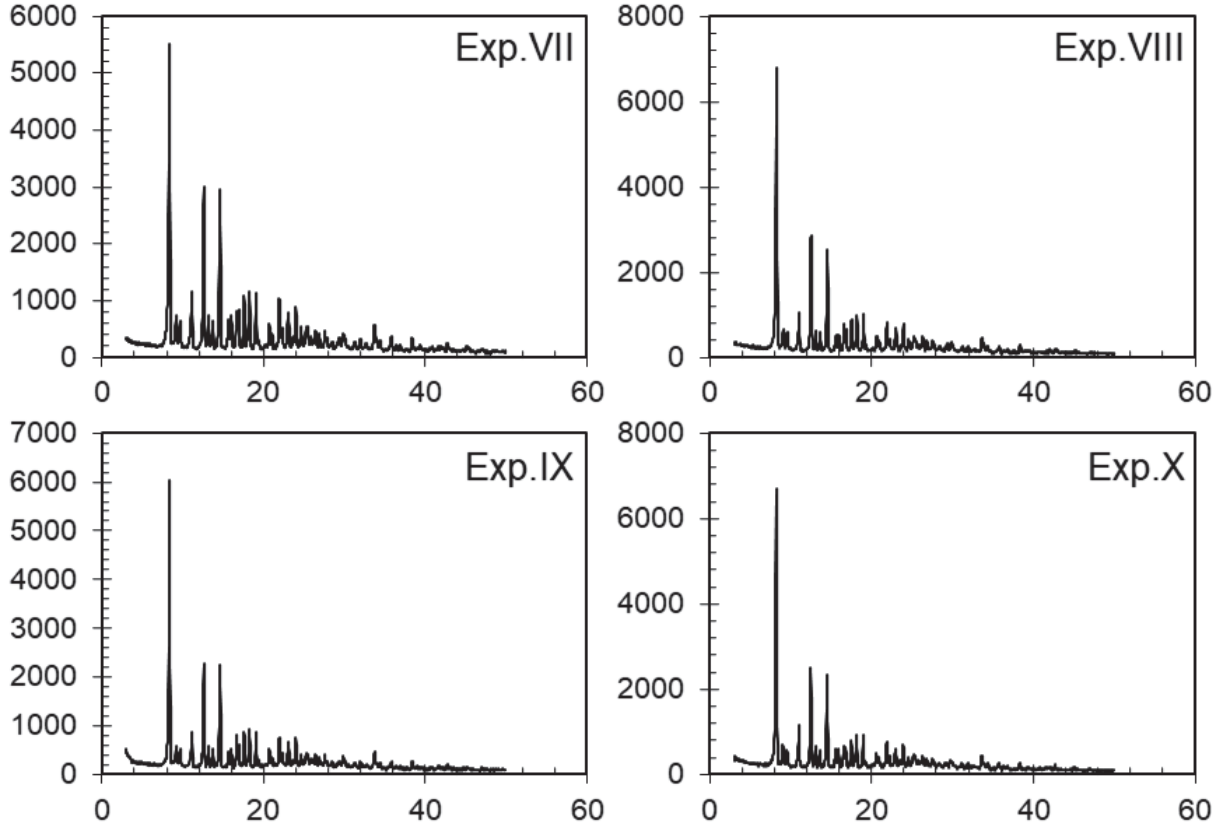

Figure S21. XRD pattern of beclomethasone dipropionate powder obtained from the integrated process. The horizontal axis is two times the angle of diffraction (2θ) and the vertical axis is the intensity.

Table S1. Ranges of operating conditions of stand- alone crystallization experiments

	Rifapentine	Beclomethasone dipropionate
Ultrasound	Applied/Not applied	Applied/Not applied
Water mass fraction API solution	0.25	0.00
Initial supersaturation (S)[a)]	1.3 – 6.0	16.0 – 147
Flow rate API solution (ml/min)	0.50 – 2.2	0.50 – 2.7
Flow rate anti-solvent (ml/min)	0.50 – 2.6	1.3 – 4.1
Flow rate nitrogen (ml/min)	0.50 – 1.5	2.2 – 3.0
Residence time (min)	30 – 240	7 – 10
Temperature (°C)	50	25 – 35
Recycling	Applied/Not applied	Not applied
Distributed anti-solvent feed	Applied/Not applied	Not applied

[a] S is defined as the ratio of the actual concentration over the saturated concentration

Table S2. Ranges of operating conditions of stand-alone spray-drying experiments

	Rifapentine	Beclomethasone dipropionate
Inlet temperature (°C)	60	75 – 90
Atomizer gas flow rate (L/h) (rotameter height (mm))	670 (55)	357 (30) – 742 (60)
Aspirator	100%	100%
Feed flow rate	2.0 ml/min	4.0 ml/min

Table S3. Ranges of operating conditions of integrated crystallization and spray-drying experiments.

	Rifapentine	Beclomethasone dipropionate
Crystallization		
Ultrasound	Applied	Applied
Initial supersaturation (S)	3.00	48.0 – 83.0
Residence time (min)	120	10
Total solution flow rate (ml/min)	4.4	4.6
Temperature (°C)	50	25
Recirculation	Applied	Not applied
Anti-solvent distribution	Applied	Not applied
Spray drying		
Inlet temperature (°C)	60	75 – 105
Atomizer gas flow rate (L/h) (rotameter height (mm))	670 (55)	357 (30) – 742 (60)
Spray drying feed flow rate (ml/min)	2.0	3.3 – 4.0
Aspirator	100%	100%

Table S4. Cut-off aerodynamic diameter of each stage in the NGI

Stage	Cut-off aerodynamic diameter (μm)	
	$Q = 99.5\ \mathrm{ml/min}$	$Q = 90.0\ \mathrm{ml/min}$
1	> 6.12	> 6.48
2	6.12	6.48
3	3.42	3.61
4	2.18	2.30
5	1.31	1.37
6	0.72	0.76
7	0.40	0.43
8	0.24	0.28

Table S5. Beclomethasone dipropionate crystallization process performance including estimated particle dimensions from SEM images

	1	**2**	**3**	**4**	**5**	**6**	**7**	**8**	**9**	**10**
Ultrasound	No	Yes	Yes	Yes	Yes	Yes	Yes	Yes	Yes	Yes
Residence time (min)	7	7	10	10	10	10	10	10	10	10
Temperature (ºC)	25	25	25	25	25	25	25	25	30	35
Initial supersaturation (S)	16.0	16.0	16.0	23.0	42.3	83.0	127	147	21.7	22.0
Yield	46%	60%	79%	89%	95%	92%	89%	76%	91%	88%
Recovery	43%	56%	72%	85%	93%	91%	89%	76%	87%	84%
Mean length (µm)	46.4	46.0	21.0	13.6	14.4	9.3	6.2	6.2	14.8	13.7
Mean width (µm)	13.9	8.1	3.8	3.8	3.3	1.5	1.4	1.1	3.4	3.8

Table S6. Yield and characteristics of aerodynamic size distribution of the crystals produced with stand-alone spray-drying experiments of beclomethasone dipropionate including estimated particle dimensions from SEM images (Figure S8).

	a	***b***	***c***	***d***	***e***	***f***	***g***	***h***	***i***	***j***
Source of crystals (see Table 6)	5	5	5	5	6	7	8	6	6	6
Inlet temperature (°C)	75	90	90	120	95	95	95	95	105	105
Atomizer flow rate (L/h)	601	601	742	742	742	742	742	357	742	357
Outlet temperature (°C)	40	50	50	68	53	55	52	56	57	62
Yield	65%	70%	72%	53%	66%	3.0%	7.8%	66%	53%	64%
EF	81%	76%	84%	68%	68%	—	56%	64%	76%	83%
FPF	22%	12%	22%	15%	35%	—	24%	16%	31%	21%
MMAD (µm)	6.9	12.2	7.6	8.4	4.9	—	10.4	7.1	4.0	6.2
GSD (µm)	3.3	4.0	5.1	3.1	2.7	—	3.8	3.1	2.7	2.9
Mean length (µm)	13	9.2	9.6	13.7	6.5	2.1	3.3	9.1	9.1	4.7
Mean width (µm)	3.3	1.9	2.9	2.9	1.9	0.79	1.1	3.0	2.7	1.7